The Sensitivity of a Coupled Atmospheric–Oceanic GCM to Prescribed Low-Level Clouds over the Ocean and Tropical Landmasses

RICHARD G. GUDGEL, ANTHONY ROSATI, AND C. T. GORDON

National Oceanic and Atmospheric Administration/Geophysical Fluid Dynamics Laboratory, Princeton, New Jersey

ABSTRACT

The sensitivity of a coupled general circulation model (CGCM) to tropical marine stratocumulus (MSc) clouds and low-level clouds over the tropical land is examined. The hypothesis that low-level clouds play an important role in determining the strength and position of the Walker circulation and also on the strength and phase of the El Niño–Southern Oscillation (ENSO) is studied using a Geophysical Fluid Dynamics Laboratory (GFDL) experimental prediction CGCM. In the Tropics, a GFDL experimental prediction CGCM exhibits a strong bias in the western Pacific where an eastward shift in the ascending branch of the Walker circulation diminishes the strength and expanse of the sea surface temperature (SST) warm pool, thereby reducing the east–west SST gradient, and effectively weakening the trade winds. These model features are evidence of a poorly simulated Walker circulation, one that mirrors a ''perpetual El Niño'' state. One possible factor contributing to this bias is a poor simulation of MSc clouds in the eastern equatorial Pacific (which are essential to a proper SST annual cycle). Another possible contributing factor might be radiative heating biases over the land in the Tropics, which could, in turn, have a significant impact on the preferred locations of maximum convection in the Tropics. As a means of studying the sensitivity of a CGCM to both MSc clouds and to varied radiative forcing over the land in the Tropics, low-level clouds obtained from the International Satellite Cloud Climatology Project (ISCCP) are prescribed. The experiment sets consist of one where clouds are fully predicted, another where ISCCP low-level clouds are prescribed over the oceans alone, and a third where ISCCP low-level clouds are prescribed both over the global oceans and over the tropical landmasses. A set of ten 12-month hindcasts is performed for each experiment.

The results show that the combined prescription of interannually varying global ocean and climatological tropical land low-level clouds into the CGCM results in a much improved simulation of the Walker circulation over the Pacific Ocean. The improvement to the tropical circulation was also notable over the Indian and Atlantic basins as well. These improvements in circulation led to a considerable increase in ENSO hindcast skill in the first year by the CGCM. These enhancements were a function of both the presence of MSc clouds over the tropical oceans and were also due to the more realistic positioning of the regions of maximum convection in the Tropics. This latter model feature was essentially a response to the change in radiative forcing over tropical landmasses associated with a reduction in low cloud fraction and optical depth when ISCCP low-level clouds were prescribed there. These results not only underscore the importance of a reasonable representation of MSc clouds but also point out the considerable impact that radiative forcing over the tropical landmasses has on the simulated position of the Walker circulation and also on ENSO forecasting.

1. Introduction

The fundamental mechanism for moist convection in the Tropics is latent heat release resulting from surface heating. At the earth's surface, the net radiative flux (shortwave + longwave) is significantly affected by the overlying clouds. Cloud impacts are particularly strong in the Tropics, where the high water vapor content renders the moist tropical atmosphere optically thicker to infrared radiation. Consequently, the surface downwelling infrared flux increases only slightly with

Corresponding author address: Dr. Richard G. Gudgel, Geophysical Fluid Dynamics Laboratory, Princeton University, P.O. Box 308, Princeton, NJ 08540.
E-mail: rgg@gfdl.gov

increasing cloudiness providing reduced compensation for the corresponding decrease in surface downward shortwave flux (Webster 1994; Ma et al. 1996; Kiehl 1998). Meleshko and Wetherald (1981) studied the impact of zonal versus a geographical distribution of clouds in an atmospheric general circulation model (AGCM). They discovered that a geographical distribution of clouds resulted in 2°–4°C surface temperature increases over the continents with corresponding decreases in surface pressure there and surface pressure increases over the oceans. Their study, however, was mostly focused on the middle latitudes and, in general, the impact of clouds over the land in the Tropics has not been extensively examined [although Meleshko and Wetherald (1981) did report significant precipitation changes in the Tropics]. In AGCM simulations,

cloud prediction errors are largely masked by the specification of sea surface temperatures (SSTs), which limit feedbacks to the atmospheric circulation. In a coupled general circulation model (CGCM), where SSTs are not specified, cloud errors over both land and ocean can have a significant local impact on surface temperatures (Stockdale et al. 1994). This is particularly troublesome due to the fact that marine stratocumulus (MSc) cloud errors are quite large in CGCMs (Ma et al. 1996).

In the Tropics, a successful simulation of the climate by CGCMs has been difficult to obtain. Among the many obstacles researchers face has been the difficulty in simulating the wind and SST seasonal cycle in the eastern tropical Pacific, weak subsidence in the eastern tropical Pacific, the maintenance of a proper SST climate (which includes the western Pacific warm pool, and the sharp east–west SST gradient across the equatorial Pacific), properly simulated monsoonal precipitation, properly timed western Pacific Madden–Julian oscillations/westerly wind bursts, and more (Mechoso et al. 1995). These deficiencies, which are also exhibited by the current Geophysical Fluid Dynamics Laboratory (GFDL) experimental prediction CGCM, represent an eastward shift in the climatologically observed position of the Walker circulation. In an effort to better understand the role that tropical MSc clouds play in regard to the CGCM deficiencies in the eastern tropical Pacific, Ma et al. (1996) and Yu and Mechoso (1999) studied tropical circulation changes brought on by the prescription of idealized seasonally varying MSc clouds near Peru in a CGCM. Gordon et al. (2000, hereafter GRG) described an effort to better simulate the eastern tropical Pacific SST and wind seasonal cycle in a CGCM by prescribing more realistic, seasonally varying climatological mean low cloud fractions over the world's oceans derived from International Satellite Cloud Climatology Project (ISCCP) data. All of these studies concluded that MSc clouds impacted not only locally on surface temperatures but also had remote effects on the central and western Pacific climate.

The weak subsidence in the eastern tropical Pacific is due, in part, to the limited ability of the CGCM's cloud prediction scheme to simulate MSc clouds. This one model deficiency alone, however, is insufficient to explain all of the model's tropical circulation problems. The failure of the CGCM to properly position the centers of tropical convection over the tropical landmasses suggests that the radiative fluxes over these regions are not reasonably simulated. Therefore, as an extension of the GRG study, observed low-level cloud fractions and optical depths over both the global oceans and tropical landmasses are specified in the CGCM. This study employs a practical approach to test the sensitivity of the CGCM to radiative forcing over the MSc region and tropical land regions. The availability of satellite-derived, low-level cloud data from ISCCP data provides a useful tool to investigate this potential

sensitivity. Certainly, there is disagreement over the optimal observation method for low-level clouds. Surface cloud observations such as Hahn et al. (1996) slightly overestimate low-level cloud amounts (Weare 1999). Satellite-based data observing systems such as ISCCP, on the other hand, have been shown to underestimate low-level clouds for a variety of reasons [the most prevalent being the covering of low clouds by overlying middle and high clouds; Hughs (1984)]. Wielicki and Parker (1992), however, found that the ISCCP algorithm *overestimates* the boundary layer cloud fraction over the oceans by about 5%. There are also discrepancies among the data observing systems concerning the very definition of a low cloud. For the ISCCP dataset, for example, a low cloud refers to a cloud having a cloud-top pressure greater than 680 hPa while the Hahn et al. (1996) dataset defines a low cloud by its maximum pressure at the cloud base. Still, Mokhov and Schlesinger (1994) stated that the ISCCP data were in much better agreement with some land-based observations than were the *NIMBUS-7* dataset studied by Hughs (1984). It seems obvious that one must carefully consider the limitations of data fields such as these. It seems reasonable, however, that as a means to test the *sensitivity* of our CGCM to both MSc clouds and low-level clouds over the land, ISCCP data are an adequate proxy.

The purpose of this paper is to study the sensitivity of a CGCM to MSc clouds and to varied radiative forcing over the tropical landmasses. To accomplish this, a number of experiments have been performed utilizing the ISCCP D2 dataset (Rossow et al. 1996). These experiments have concentrated on three issues: the impact of MSc clouds on El Niño–Southern Oscillation (ENSO) predictability, the sensitivity of the Walker circulation in a CGCM ensemble annual mean to low clouds over the tropical landmasses, and the interaction, if any, between them. The model's sensitivity to the specification of ISCCP low-level clouds over just the global oceans (which would include, of course, MSc clouds) versus over the global oceans plus the tropical landmasses is of particular interest. The first experiment will consist of clouds that are fully predicted by the CGCM. The second experiment will include forcing from ISCCP low-level clouds over the global oceans. The third experiment will include forcing from ISCCP low-level clouds over the global oceans and over the tropical landmasses.

Section 2 describes the atmospheric and ocean models, the coupling method, and experimental design. Section 3 examines sensitivity of the CGCM to ISCCP low-level cloud forcing. A detailed discussion of the effect of prescribed clouds on the Walker circulation among the experiment sets is given in section 4. Section 5 shows how these changes affect the coupled model's ability to hindcast ENSO. A summary of results and conclusions is presented in section 6.

2. Model description

a. The oceanic model

The configuration of the oceanic general circulation model (OGCM) is similar to that described in Rosati et al. (1997). The model equations are solved on a nearly global grid with realistic topography using the Modular Ocean Model version 2 (MOM2) (Pacanowski 1995). The model has 1° longitudinal resolution, and variable latitudinal resolution of 1° from 78°S to 64°N except for a 1/3° resolution from 10°S to 10°N. The model has 15 unequally spaced vertical levels [specified to resolve the upper ocean; see Derber and Rosati (1989)] and utilizes a Richardson number–dependent vertical mixing scheme (Pacanowski and Philander 1981). The horizontal mixing was adapted from the Smagorinsky nonlinear viscosity (Smagorinsky 1963). The parameterizations also include penetration of solar insolation into the ocean subsurface.

b. The atmospheric model

The AGCM employed here is a global spectral model (see GRG). The horizontal resolution is T42 (as opposed to T30 in GRG) where T42 denotes a Gaussian grid of ~2.8125° longitudinal resolution by 2.8125° latitudinal resolution. The model has 18 vertical levels. For experiments involving prescribed ISCCP low-level clouds, a method similar to the one described in GRG is implemented. This method utilizes interannually varying, monthly diurnal mean ISCCP D2 data (Rossow et al. 1996), which is linearly time interpolated to radiation time steps for insertion into the CGCM. The monthly diurnal mean low cloud fraction is computed using

$$low = total - high - middle, \qquad (1)$$

where total, high, and middle denote the ISCCP D2 monthly diurnal mean total, high, and middle cloud fractions, respectively. Equation (1) is consistent with the overlap assumptions used to generate the ISCCP D2 IR-marginal total cloud amount. ISCCP cloud-top pressure data are employed to position the ISCCP low clouds within the vertical column. There are, however, some differences from the method employed by GRG that are directly related to cloud-radiation issues. First, wherever low-level cloud fractions are specified from the ISCCP D2 dataset, low cloud optical depth is also derived from this dataset. In contrast, in GRG, a fixed value, that is, 9.0, was used for low-level optical depth. Hereafter, the expression low-level clouds shall refer to the combination of low cloud fraction and low cloud optical depth. Second, interannually varying monthly mean low-level clouds are prescribed over the global oceans and, in the experiments where land clouds are specified, climatological (1984–93) monthly mean ISCCP low-level clouds are prescribed over the land. This differs from GRG in that climatological ISCCP low-level clouds were prescribed only over the global oceans. Third, di-

urnally varying solar radiation is implemented. Among the other differences between the present CGCM and that used for GRG, the relaxed Arakawa–Schubert parameterization of cumulus convection (Moorthi and Suarez 1992) is now employed instead of the full Arakawa–Schubert scheme used by GRG.

c. The coupled forecasting system

The AGCM and OGCM were coupled every 2 h. The atmospheric model had a time step of 800 s and the radiation calculation was performed every 2 h. The 2-h atmospheric averages of heat flux, wind stress, and precipitation minus evaporation were calculated and used to force the ocean model. The OGCM, which had a 1-h time step, was then run to provide 2-h average SST values, which could then be used for the next 2 h of atmospheric model integration. The atmospheric initial conditions utilized in all experiments were obtained from a long time-integrated AGCM run forced with prescribed SSTs. The ocean initial conditions came from an ocean data assimilation (Rosati et al. 1994).

d. Experimental design

An ensemble of ten 12-month CGCM forecasts was run for the period 1984–93 in order to investigate the impact of specified ISCCP low-level cloud forcing upon the simulated tropical circulation and upon seasonal ENSO forecasting skill. The 12-month forecast length allows for the exploration of the model's mean state response over timescales relevant to the seasonal prediction problem and the study of ENSO forecast skill in a time frame extending out to 1 yr. The ensemble annual mean (hereafter referred to as EAM) can then be used as a measure of the model's background state and thus can quite nicely depict model strengths and deficiencies during a time period relevant to the seasonal prediction problem. All experiments were initialized from 1 January 0000 UTC.

Five different CGCM experiments were run. The first CGCM experiment, the Control Model experiment (CM), utilized a diagnostic cloud prediction scheme (GRG) and represents a method employed frequently for seasonal to interannual prediction at GFDL. This scheme predicts cloud fractions over both ocean and land and places the clouds in up to three layers (low, middle, and/or high) of the atmosphere. The algorithm for MSc clouds, however, which is described in detail in GRG, inadequately predicts MSc clouds due, in part, to deficiencies such as a lack of prognostic cloud water, incomplete representation of mixing processes across inversions, insufficient detailing of microphysical processes such as cloud drizzle, etc. The second CGCM experiment (CMIO) differed from experiment CM in that prescribed interannually varying monthly mean ISCCP D2 low-level clouds replaced the model-predicted low-level clouds *over the global oceans.* The

TABLE 1. Experimental design.

Exp.	Prescribed ISCPP low-level clouds
CM	No
CMIO	Yes (global ocean)
CMIOL	Yes (global ocean and land clouds from 15°S to 15°N)
CMIOLW	Yes (global ocean and land clouds from 15°S to 15°N Western Hemisphere only)
CMIOLE	Yes (global ocean and land clouds from 15°S to 15°N Eastern Hemisphere only)

third CGCM experiment (CMIOL) differed from CMIO in that prescribed climatological monthly mean ISCCP D2 low-level clouds (calculated from the 1984–93 time period) replaced the predicted low-level clouds over all land regions between 15°S and 15°N. Two auxiliary experiments were run that differed from CMIO in that prescribed climatological monthly mean ISCCP low-level clouds were prescribed over land regions between 15°S and 15°N only over the Eastern Hemisphere, west of the date line (CMIOLE) and only over the Western Hemisphere, east of the date line (CMIOLW), respectively. The complete experiment set is depicted in Table 1.

3. CGCM EAM and seasonal cycle sensitivity to ISCCP low-level cloud prescription

The difficulty that the diagnostic cloud prediction scheme has in predicting low-level stratus clouds is depicted in Fig. 1, which shows the mean 1984–93 low-level cloud fractions from ISCCP and the EAM from the CM experiment (note that the EAM value contains forecasts for months 1–12; for each of the total of 10 individual forecast years and, thus, encompasses various leads and seasons). A comparison of the mean 1984–93 MSc clouds (see Figs. 1a,b) shows that some MSc clouds are evident in the CM but are markedly fewer in both areal coverage and cloud fraction than is found in ISCCP. For example, the low-level cloud fractions in the eastern tropical Pacific exceeds 60% over a large portion of this region in ISCCP whereas the CM experiment low-level cloud fractions exceed 50% for a much smaller portion of this region. In fact, cloud fractions as low as 10% can be found along the coast of South America near 20°S. It is also notable that the CM experiment poorly simulates the seasonal cycle of MSc clouds (not shown) and produces much more low-level cloud cover over most tropical land regions as compared to the ISCCP dataset.

In Fig. 2, the EAM net radiative fluxes at the top of the atmosphere (TOAnet) generated by the CM, CMIO, and CMIOL experiments are compared with observed values taken from the Earth Radiation Budget Experiment (ERBE; Barkstrom et al. 1990). In the ERBE dataset (see Fig. 2a), three distinct regions of maximum TOAnet can be found in the Tropics. The first is over central Africa. The second region extends from the Indian Ocean all the way to the western tropical Pacific Ocean (this includes the Indonesian Archipelago). The third region can be noted extending from the Amazon basin eastward across the tropical Atlantic Ocean. A sharp gradient of TOAnet is evident extending from the Amazon basin southwest across the Andes to the MSc
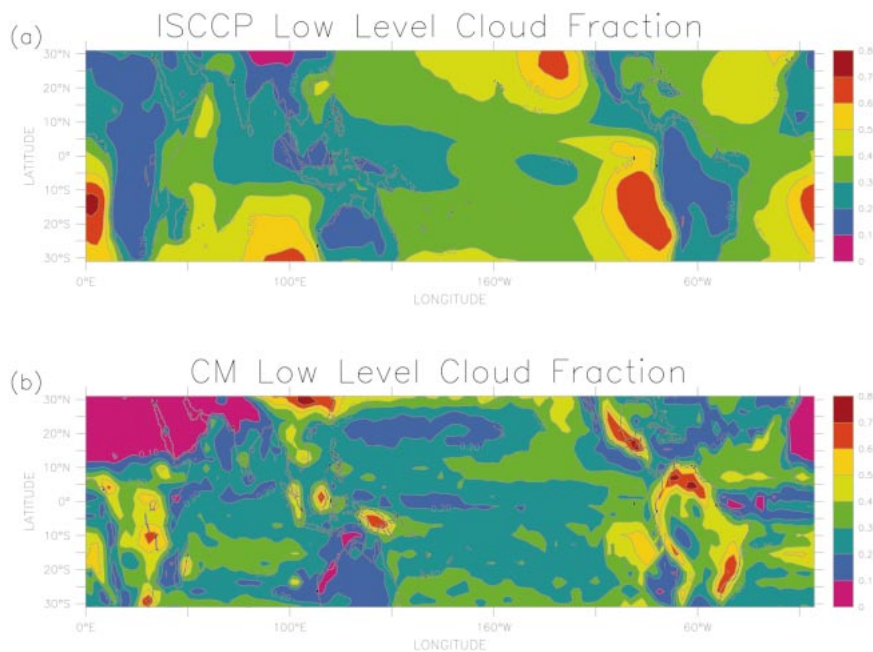
FIG. 1. Comparison of ISCCP low-level clouds with model-predicted clouds. Shown are 1984–93 10-yr mean (ISCCP) and EAM (ten 1-yr averages) cloud fractions for (a) ISCCP and (b) CM.
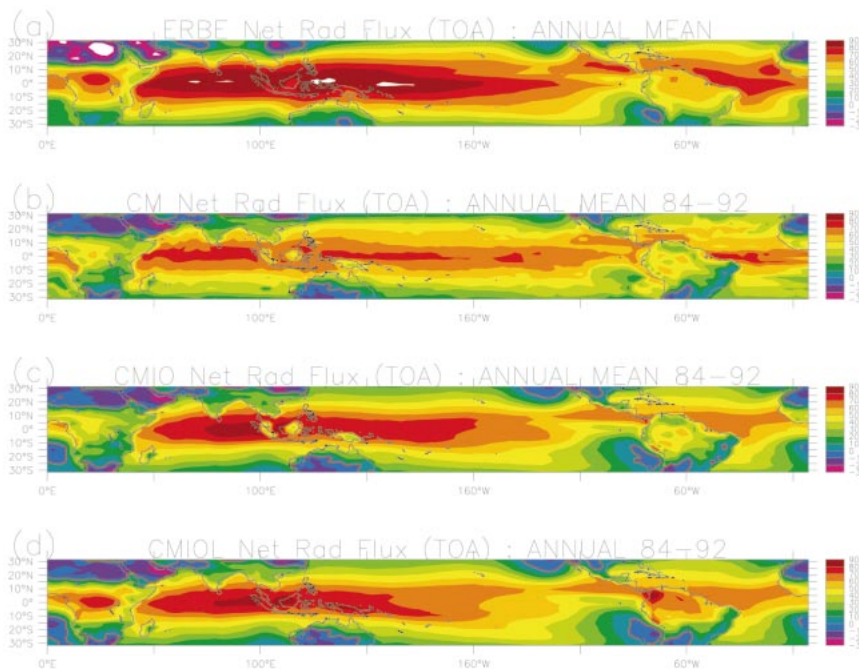
FIG. 2. Net radiation at the TOA, defined as TOA shortwave down minus TOA shortwave up minus OLR in W m^{-2} for (a) annual mean observations taken from the Earth Radiation Budget Experiment, (b) CM EAM, (c) CMIO EAM, and, (d) CMIOL EAM.

region over the waters just west of Chile (hereafter referred to as the Amazon–Chile TOAnet gradient).

In Fig. 2, one can note that all three experiments underpredict TOAnet over the Indian and western tropical Pacific Oceans. The results do, however, show a clear relationship between the underprediction of MSc clouds in the eastern tropical Pacific and excessive TOAnet in the CM experiment. One can also note that excessive low-level cloud cover over the Indonesian Archipelago corresponds to underestimates of TOAnet. In this experiment, the regions of maximum TOAnet are all centered over the oceans and the African maximum and the Amazon–Chile TOAnet gradient are poorly simulated. A significant underestimate of TOAnet ($\sim$50 W m^{-2}) is also evident over the land regions in the Indonesian Archipelago. In the CMIO experiment, one can note more realistic TOAnet values over the Indian Ocean and in the eastern tropical Pacific MSc region (evidence of the impact of the prescribed MSc clouds from ISCCP). The Amazon–Chile TOAnet gradient, however, is weak due to the underestimate of TOAnet over the Amazon basin. One can also note that the CMIO experiment, similar to the CM experiment, underestimates TOAnet over central Africa and the land regions of the Indonesian Archipelago. The CMIOL experiment, on the other hand, although not perfect in magnitude or precise location, does a much better job in capturing the position and strength of the regions of maximum TOAnet that are found in observations. Over central Africa, the CMIOL TOAnet values compare

quite well to those found in observations. TOAnet values in the western portion of the Indonesian Archipelago (near Sumatra) are underestimated by about 10 W m^{-2} while Borneo and New Guinea are showing overestimates of about 10 W m^{-2}. Over the Amazon basin, although the CMIOL overestimates TOAnet, the resulting gradient across the Andes to the MSc region west of Chile is more realistic than the gradient found in the other two experiments. In short, while not perfect, TOAnet patterns show significant improvement in the CMIOL experiment. These improvements are particularly notable over central Africa and the Indonesian Archipelago while over tropical South America it is the Amazon–Chile TOAnet that is improved and not so much the total TOAnet, which is now stronger than is found in observations. The explanation for this difference in sensitivity is still an open question. It may be noted that changes in low-level cloud can induce changes in middle- and/or high-level clouds. In turn, these changes could then contribute to CMIO and CMIOL radiative responses.

The inability of the CM model to simulate reasonable MSc clouds results in warming of the SSTs in the eastern tropical Pacific and contributes to the reduction in the east–west SST gradient across the equatorial Pacific. In the western tropical Pacific (see Fig. 3, upper-left panel), CM has a cold bias in temperature of $-2°$C, which reduces the expanse of the western Pacific warm pool. In the eastern tropical Pacific, a warm bias (over 3°C in spots) occurs. Both ISCCP-prescribed experiments
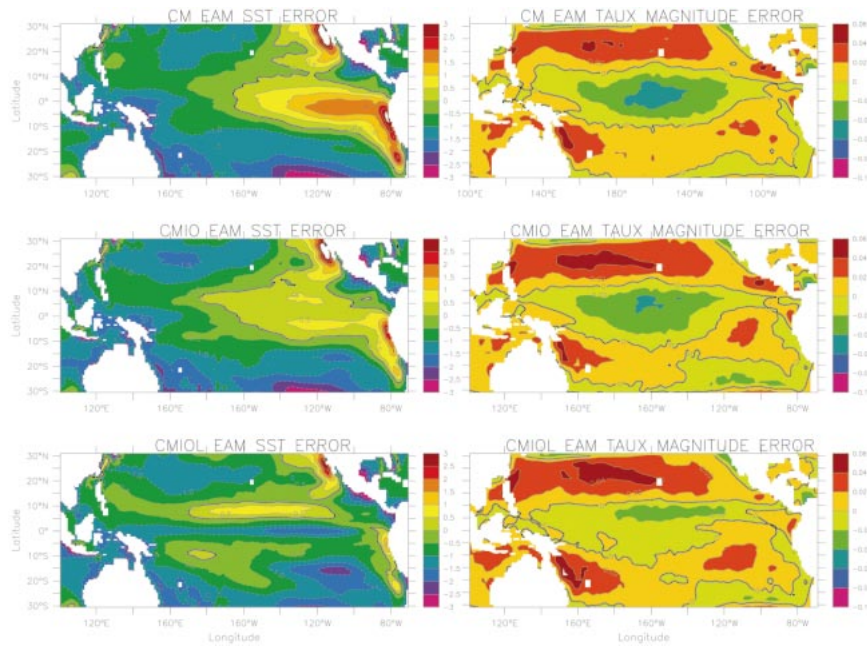
FIG. 3. A comparison of EAM SST and zonal wind stress differences with observations (Reynolds 1988). The upper-middle and lower-left panels represent the EAM SST differences in °C taken from the 1984–93 EAM's for the CM, CMIO, and CMIOL experiments, respectively. The upper-, middle-, and lower-right panels represent the zonal wind stress magnitude differences in N m^{-2} for the CM, CMIO, and CMIOL experiments, respectively.

have improved EAM values, but the CMIOL simulation is markedly better than CMIO. In the western tropical pacific, the SST cooling error is improved in the CMIOL experiment as is the erroneous warming in the eastern tropical Pacific. The CMIOL experiment also shows strengthened trade winds (see Fig. 3, right panels), which more closely approximates those found in observations. All of these improvements serve to reduce (in the CMIO experiment) or essentially eliminate (in the CMIOL experiment) the erroneous displacement of the western Pacific warm pool eastward during the 12-month forecast. This last feature of the coupled system was one that had previously produced a model (i.e., CM) whose mean EAM closely resembled an El Niño state.

This tendency of the CM and (to a lesser extent) the CMIO experiments to relax the trades and erroneously displace the western Pacific warm pool eastward can be noted in Fig. 4, which depicts the 1984–93 mean annual cycles of SST and surface zonal wind stress at the equator from observations and from the CM, CMIO, and CMIOL experiments, respectively. It is also notable that the CMIOL experiment maintains the warmest waters to the west of the date line throughout the seasonal cycle and that its seasonal cycle of surface wind stress more reasonably approximates that of the observed surface wind stress. Such results are not the case for either the CM or CMIO experiments. The magnitude of the CMIOL zonal wind stress, when compared to the magnitude of the observed climatological zonal wind stress (Legler and O'Brien 1988), is also well simulated. Both

CM and CMIO have weakened trades. In the eastern tropical Pacific, the meridional component of wind stress (not shown) is too strong for the first 6 months of all three experiments. For the last 6 months (Aug–Dec), CM meridional wind stress weakens while CMIO and CMIOL both remain strong. The seasonal variability, however, is slightly weak in all three simulations—most notably in the failure to properly weaken the springtime southerlies in the eastern tropical Pacific. However, the phase of the maximum southerlies is delayed in both the CMIO and CMIOL experiments (as compared to the CM experiment), in better agreement with observations and consistent with the results of GRG.

It has been shown that, as a consequence of specifying both the global ocean and tropical land low-level clouds, there are distinct improvements to the tropical EAM. The CMIOL SSTs and wind stress, as well as precipitation (not yet shown), are all more realistic. The convective centers, as represented by the regions of maximum TOAnet, appear to be situated in more reasonable locations. In the next section, a closer look at the model-simulated tropical EAM and, in particular, the impact of the changed radiative forcing over the tropical landmasses on the simulated Walker circulation will be discussed.

4. The EAM Walker circulation

The intensification and shift in the location of the centers of tropical convection are an essential element
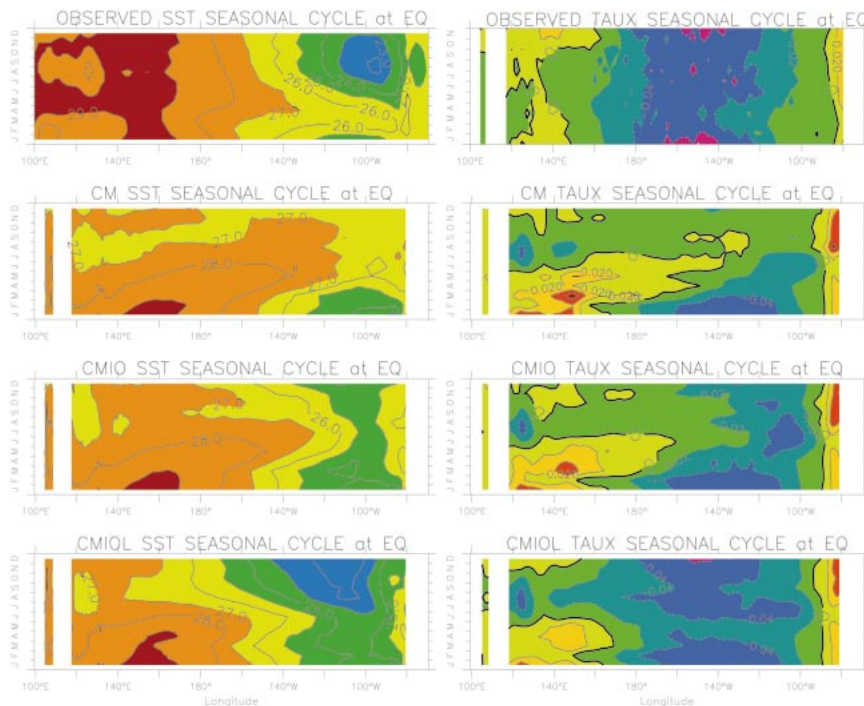
FIG. 4. A comparison of the 1984–93 mean seasonal cycle of SST and zonal wind stress at the equator. Shown are the observed Reynolds' climatological SSTs and the CGCM SSTs in °C from CM, CMIO, and CMIOL in the upper, second from top, second from bottom, and bottom left panels, respectively. The corresponding zonal wind stress fields in N m^{-2} are shown in the panels on the right.

of the response of the simulated EAM tropical circulation to the prescribed climatological monthly mean low-level clouds over land in the CMIOL experiment. It should be noted that these responses correspond to shifts of the centers of maximum TOAnet. Also, in this experiment, both the 1000-mb divergence and precipitation fields (not shown) show a strengthening of tropical convective activity over the tropical land regions and a stronger, more realistic ITCZ than does either the CM or CMIO experiments.

Another way to measure the magnitude of the differences in the tropical circulation among the experiments is to quantify the Walker circulation (which consists of the Pacific cell and its companion cell over the Indian Ocean) strength and position in each experiment. The strength of the Walker circulation can be diagnosed by calculating the deep equatorial circulation in the longitude–height plane. Utilizing the formulation of Newell et al. (1974), the ''zonal mass flux'' is:

$$M(p) = \frac{r_e}{g} \Delta\phi \int_{p_s}^{p} U' \, dp,$$

where M measures the strength of the Walker circulation. In the above equation, r_e is the radius of the earth, g is gravity, $\Delta\phi$ is a latitude increment ($=10°$), and U' is the eddy zonal wind (i.e., the zonal wind minus its zonal mean) averaged over a latitude band of 5°S–5°N.

This value, in conjunction with the U and W (i.e., the zonal and vertical) components of the wind, defines not only *where* the main regions of upward and downward flow reside in the model, but also the *overall strength* of the circulation. Figures 5a and 5b show M (contoured), the wind vectors in the longitude–height plane (hereafter referred to as $U–W$), and the U value (shaded) for experiments CMIO and CMIOL. (Note: the CM experiment results for these variables are not shown since they look very similar to the CMIO results.) Looking at the vertical cross sections shown in Fig. 5, one can discern the circulation pattern representing the Pacific cell of the Walker circulation (which rotates clockwise). The companion cell over the Indian Ocean, rotating counterclockwise, is not as obvious but consists of rising motion over the eastern Indian Ocean and descending motion over the region west of Africa near 10°W. Over the Pacific, one can note that the descending branch in the eastern Tropics is stronger in the CMIOL experiment than in the CMIO experiment. The M values, whose extrema indicate where U' changes sign, are also notably stronger in the CMIOL experiment to the west of the Andes both near the surface and aloft. In the western tropical Pacific, ascending motion over the land is stronger and centered over the Indonesian Archipelago in the CMIOL experiment while a weaker and much broader region of upward vertical motion is evident in the CMIO
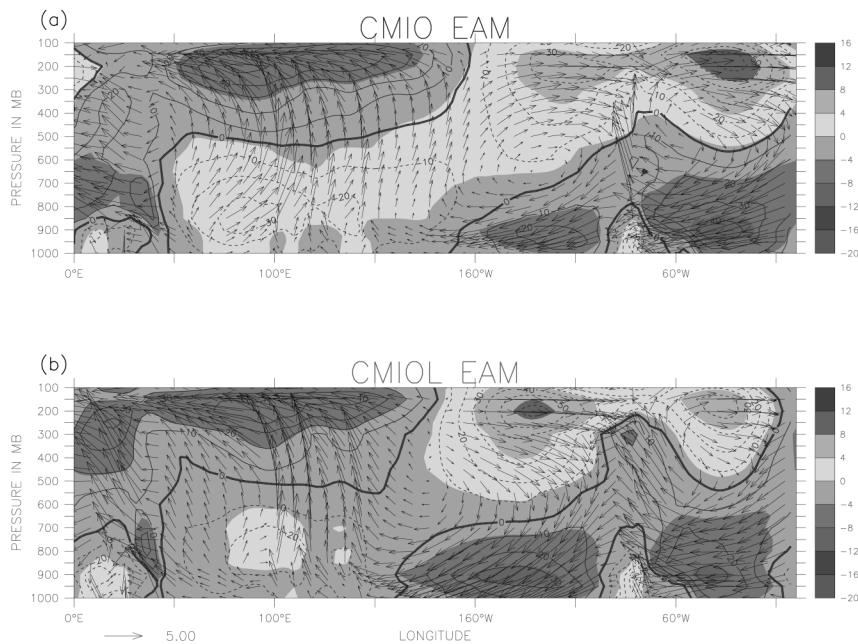
FIG. 5. The 5°S–5°N averaged cross sections showing a comparison of EAM averages (CMIO and CMIOL) from 1984 to 1993. Variables shown in each frame include U in m s^{-1} (shading), wind vectors in the longitude–height plane (U–W) with W in 0.01 m s^{-1}, and zonal mass flux (contours) in 10^9 kg s^{-1}. Shown are (a) CMIO and (b) CMIOL.

experiment. Thus, the CMIOL experiment has produced a more focused region of organized upward motion centered over the land whereas the CMIO experiment, on the contrary, shows a much more diffuse region of upward vertical motion that extends considerably farther eastward over the Pacific Ocean.

This figure also shows some interesting features over the Atlantic and Indian Ocean basins. One can note a third tropical circulation cell, rotating clockwise, over the Atlantic basin consisting of strong upward vertical motion over South America and descending motion in the eastern tropical Atlantic. For the CMIOL experiment, the circulation of this cell appears to be weaker than found in the CMIO experiment both at the surface and aloft. Over the Indian Ocean basin, upward vertical motion is weaker in the eastern part of the basin for the CMIOL experiment. The descending motion near 10°W is also weaker than that found in the CMIO experiment. Thus, the CMIOL has produced a strengthened east–west vertical circulation pattern over the Pacific Ocean and weaker patterns over the other two basins.

Using data from the European Centre for Medium-Range Weather Forecasts (ECMWF), Webster (1994) portrayed the shift in the Walker circulation between an El Niño and a non–El Niño year in zonal cross sections similar to those shown here. If one examines the two vertical sections along the equator for 1985 and 1987 from Webster (1994) and compares them to the CGCM U–W fields shown in Fig. 5, it is quite apparent that the EAM U–W from the CMIO experiment closely resembles that seen in 1987, which was an El Niño year. As

was mentioned earlier, CMIO, and especially the CM experiment, both have EAM SSTs and surface winds in the Tropics whose patterns closely resemble that of an El Niño. A further proof of this bias can be noted in the Walker circulation of CMIO (see Fig. 5a) and is also evident in CM (not shown).

Since the CGCM is extremely sensitive to changes in the radiative forcing imposed upon all land regions in the Tropics, one can ask whether or not these results might be qualitatively duplicated by restricting the ISCCP low-level cloud prescription over the land to only "portions" (select regions) of the Tropics. To explore this question, two auxiliary experiments, CMIOLE and CMIOLW, were run in which clouds were prescribed only over a portion of the tropical landmasses (i.e., only in the Eastern or Western Hemisphere, respectively). The results, shown in Figs. 6a–c, which represent the equatorial U–W and atmospheric temperature differences of the land cloud prescribed experiment versus the CMIO experiment, indicate that prescribing clouds only over a portion of the tropical land areas is insufficient to produce the marked responses notable in the CMIOL experiment. In Fig. 6a, which depicts the CMIOLE–CMIO U–W and temperature differences, one can note that the ISCCP low-level cloud prescription over the Indonesian Archipelago and Africa has intensified the overall strength of the Pacific Walker cell and weakened the circulation of the Indian cell (note that the *clockwise* flow aspects of these differences represent a *weakening* and not a strengthening of the *counterclockwise* flow of the Indian cell). The magnitude of
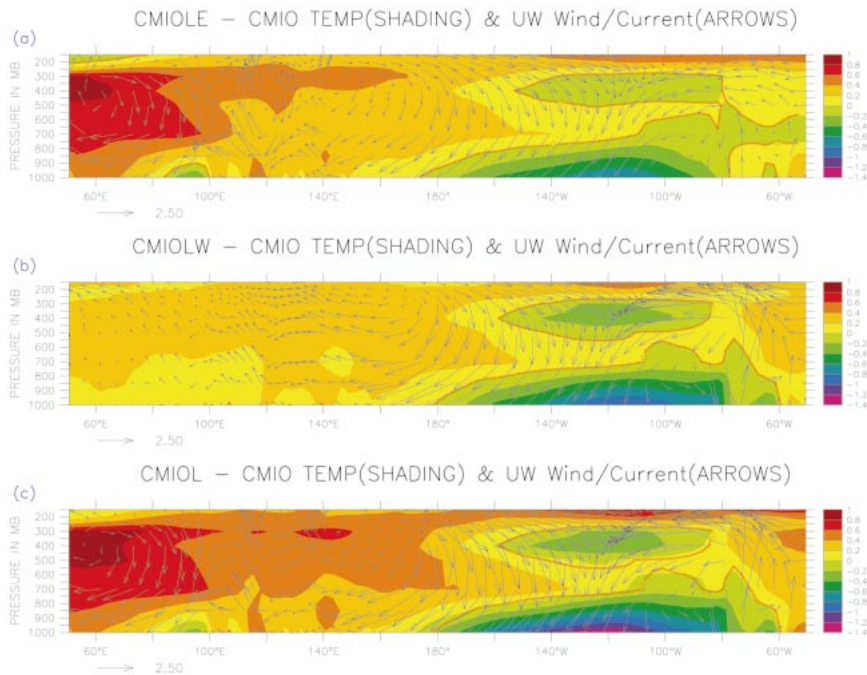
FIG. 6. EAM cross sections at the equator. Shown are three land cloud–forced experiments differenced with CMIO. Variables depicted include temperature differences in °C (shading) and U–W (vectors). The U units are m s^{-1} for atmospheric zonal wind; W units are 0.01 m s^{-1} for atmospheric vertical velocity. Shown are (a) CMIOLE–CMIO, (b) CMIOLW–CMIO, and (c) CMIOL–CMIO.

these changes, however, is not quite as large as that found in the CMIOL experiment. Over the Atlantic, the differences between CMIO and CMIOLE are much smaller than those between CMIO and CMIOL. In Fig. 6b, which depicts the CMIOLW–CMIO differences, it is now the circulation cell over the Atlantic Ocean (weakened) and the Pacific Walker cell (strengthened) that have been impacted by the ISCCP cloud prescription. Thus, it appears that the ISCCP low-level clouds over the tropical landmasses have a greater impact on the overlying circulation cell and less impact on the remote cell. In addition, these experiments indicate that the Walker circulation is closely linked to a third cell that is situated over the Atlantic Ocean. One can conclude that the strength and position of these equatorial east–west vertical cells are a function of the radiative forcing not only over the ocean surface but also over the tropical landmasses.

5. ENSO hindcast skill in the CGCM

As previously discussed, the prescription of ISCCP low-level clouds over the ocean alone produced only modest EAM improvement whereas the expansion of the cloud prescription to the adjacent land regions (in the Tropics) produced a marked improvement. Does the improvement to the model's EAM come at the "expense" of model interannual variability and thereby have little or no effect on the hindcast skill for the first year?

In Fig. 7a, the ENSO hindcast skill in the Niño-3 region (which is the domain 5°S–5°N and 150°–90°W) is displayed. ENSO hindcast skill is determined by correlating Niño-3 SST anomalies, calculated from each experiment's EAM, with observed anomalies (Reynolds 1988). It should be noted that the observed ISCCP low-level clouds *over the oceans* contain information on interannual variability that would not be available for a true forecast. The motivation for this work, however, was to investigate the impact of MSc clouds on ENSO prediction as well as the impact, if any, of low-level clouds over the tropical land regions on the tropical environment. The former asks the question, "If one could reasonably predict MSc clouds, would that improve ENSO prediction?" The latter asks the question, "Do the radiative processes over the tropical landmasses also have an impact on ENSO prediction?" Figure 7a shows that CMIO does result in improved skill scores relative to CM, which indicates that the MSc clouds have indeed positively impacted on the ability of the model to predict ENSO. In contrast, when *climatological* monthly mean ISCCP low-level clouds were prescribed over the global oceans, the skill scores from this experiment (not shown) were similar to the skill scores from the CM experiment and thus were quite poor. This highlights the importance of capturing the interannual
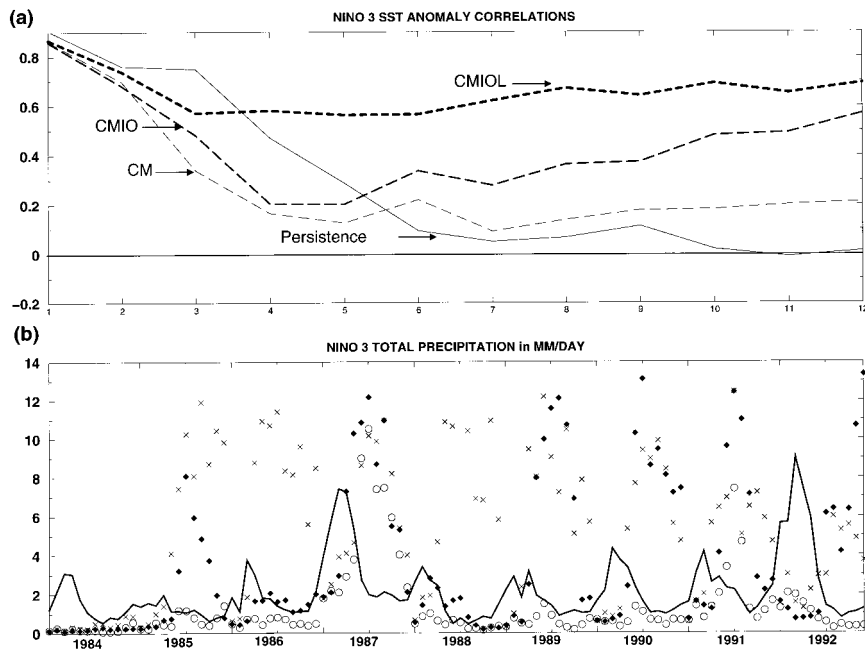
FIG. 7. (a) Computed Niño-3 SST anomaly correlations through time (12-month forecast) for the time period 1984–93. Shown are persistence (thick solid line), CM (thin solid line), CMIO (thick dashed line), and CMIOL (thick dotted–dashed line) for Niño-3 SST correlations vs Reynolds' observed SSTs. (b) Niño-3 total precipitation in mm day^{-1}. Shown are observations (thick solid line), CM (Xs), CMIO (filled diamonds), and CMIOL (circles).

variability of the MSc clouds for successful ENSO prediction. One might think that since the entire Niño-3 region lies within the Pacific, the impact of the prescribed clouds over the Pacific would dominate *both* the CMIO and CMIOL SSTs. This is not the case, however, as the CMIOL experiment shows considerably more skill than the CMIO experiment throughout the *entire* 12-month hindcast period. Thus, ENSO prediction is sensitive to the radiative processes over the tropical landmasses.

When one examines the precipitation fields from Niño-3 for each experiment (Fig. 7b), it can be noted that CMIOL has the most realistic simulation of precipitation when compared to the other experiments. The CM experiment, with the lone exception of 1984, predicts much more precipitation than is found in observations and also shows very little interannual variability. As was discussed previously, such a bias is the result of an improperly positioned Walker circulation, which is an essential element for correctly simulating AGCM SST–cloud feedbacks. The CMIO experiment, on the other hand, does perform well for some of the years in the 1980s (1984, 1986, 1987, and part of 1988) but performs poorly in 1985 and from 1989 to 1993. Similarly, both the CMIOLE and CMIOLW experiments outperform the CM experiment but still miss many more years than does the CMIOL experiment (not shown).

It is well known that the observed Walker circulation fluctuates, on the ENSO timescale, from strong to weak phases. A strong Walker circulation (La Niña) is as-

sociated with colder than normal SSTs and stronger than normal descending motion and trade winds in the eastern tropical Pacific, and strong ascending motion over the Indonesian Archipelago. A weak Walker circulation (El Niño) is associated with warmer than normal SSTs in the eastern tropical Pacific and weak (or even reversed) trade winds. During an El Niño event, the ascending motion in the western tropical Pacific is still evident over the Indonesian Archipelago but is weaker than that which is found under La Niña conditions. Also, during El Niño conditions, the region of ascending motion over the Indonesian Archipelago extends eastward over the western tropical Pacific Ocean (which coincides with the movement of warm SSTs eastward and the spread of surface westerlies) and the upper-level westerly flow in the eastern tropical Pacific weakens considerably. Thus, the Walker circulation can be measured by noting both the *intensity* and *position* of the ascending and descending branches of the circulation in the tropical Pacific. These changes in the intensity of the tropical circulation in the equatorial Pacific (and the corresponding shift in position of the ascending and descending branches) are quite discernible in the ECMWF assimilation [see Webster (1994) for the 1982/83 El Niño and 1985 La Niña]. The features are also quite notable in the CMIOL experiment. In Fig. 8, the U (shading), U–W (vectors), and M (contours) values are shown for the contrasting warm and cold events of the 1987 El Niño/1988 La Niña from the CMIOL hindcasts. These fields reveal that the CMIOL experiment
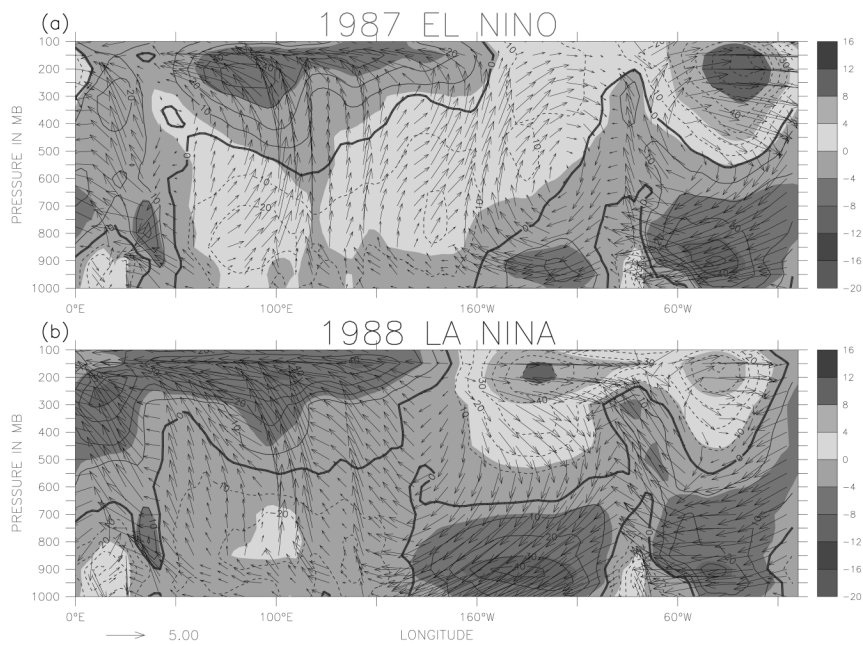
FIG. 8. The 5°S–5°N averaged cross sections of U in m s^{-1} (shading), wind vectors in the longitude–height plane (U–W) with W in 0.01 m s^{-1}, and zonal mass flux (contours) in 10^9 kg s^{-1}. Shown are (a) CMIOL 1987 El Niño EAM and (b) CMIOL 1988 La Niña EAM.

predicted the fluctuations of the Walker circulation from El Niño conditions (1987, Fig. 8a) to La Niña conditions (1988, Fig. 8b). The CMIO experiment, on the other hand, fails to predict the key elements notable during the 1988 La Niña (not shown).

The separation in simulated precipitation between the CMIO and CMIOL experiments for the 1990s highlights a persistent problem of lowered hindcast skill during this decade for the GFDL CGCM. The inclusion of the ISCCP low-level clouds over the land, as it turns out, was a necessary condition for model skill in the 1990s. This is evident in the more realistic simulation of precipitation in the CMIOL experiment in the Niño-3 region and is also shown by the improved skill scores. Prior to the present study, all attempts to forecast ENSO in the 1990s had low skill using this CGCM. CMIOLE and CMIOLW experiments seem to have success in hindcasting precipitation in the 1990s but, interestingly, do poorly in the 1980s (not shown). These features might be pointing toward decadal changes in ENSO regimes (such as an ENSO regime mostly driven by a delayed oscillator mode as compared to one that is more stochastically driven). Although it is beyond the scope of this paper to investigate this issue further, these results do hint at changes in the sensitivity of the eastern tropical Pacific to radiative fluctuations over the tropical landmasses not only from one region of the Tropics to another but also from one decade to the next.

6. Summary and conclusions

This study examined the sensitivity of a CGCM system to prescribed ISCCP low-level clouds and low-level optical depths obtained from the ISCCP D2 data source. A T42L18 atmospheric model coupled to a modified MOM2 oceanic model with 15 levels was utilized to perform this study. Applying an approach resembling that described in GRG, both global ocean-only and global ocean and tropical (15°S–15°N) land clouds were prescribed into the lowest cloud levels for the time period 1984–93. Three CGCM experiments (CM, with fully predicted clouds; CMIO, with ocean-only ISCCP cloud prescription; and CMIOL, with both ocean and land ISCCP cloud prescription) consisting of ten 12-month runs were performed. The results indicate that the addition of the ISCCP low-level tropical land clouds led to a more realistic positioning of the regions of maximum convection in the Tropics and was therefore essential for the simulation of the tropical EAM circulation in the first year. The increased TOAnet over key land regions in the Tropics (Africa, the Indonesian Archipelago, and South America) combined with the cooling effect of the MSc clouds is consistent with this result. The elimination of any of the key tropical land regions from the cloud prescription dataset degraded the results indicating that an accurate representation of the radiative fluxes over *all* the tropical landmasses is needed for the simulation of the tropical circulation. The most pronounced improvement shown in these experiments in the EAM circulation could be noted in the strength and position of the Walker circulation. Other EAM improvements resulting from the land and ocean low-level cloud prescription included stronger trades, a more well-defined and well-positioned ITCZ and South Pacific convergence zone, and improved precipitation

patterns in the Tropics. The CM experiment had a strong bias toward a tropical regime mirroring an El Niño state. It showed marginal skill in ENSO prediction. CMIO (with interannually varying MSc clouds) was successful in improving ENSO hindcast skill but not to the extent of CMIOL.

This leads to the following conclusions for this CGCM study.

1) Tropical marine stratocumulus clouds are an essential feature of the tropical climate and interannual variability, both of which must be reasonably captured in order to achieve skill in ENSO prediction.
2) The strength and position of the Walker circulation is a function of the radiative forcing not only over the ocean surface, including the MSc region, but also over the tropical landmasses.
3) The Walker circulation must be reasonably positioned in order to successfully capture the nonlocal feedback effect of MSc clouds. For example, a proper positioning of the region of subsidence in the eastern tropical Pacific is a necessary condition for optimal simulation of MSc cloud feedbacks.
4) Reducing a CGCM systematic bias (in this case, an improperly positioned Walker circulation), combined with reasonable interannually varying MSc clouds over the ocean, yields a considerable improvement in ENSO hindcast skill in the first year.

The fourth conclusion answered a not-so-obvious question concerning the impact of reducing model biases on model forecasting skill. In this study, a reduction in a CGCM systematic error (whereby a model bias of shifting the Pacific Walker cell eastward is mollified) did, in fact, lead to an improvement in the model's ENSO variability.

Several questions remain unanswered, however, and will be the emphasis of further research. Over central Africa and the Indonesian Archipelago, the GFDL CGCM overpredicts low cloud fraction. The prescription of the ISCCP low-level clouds greatly ameliorated this problem resulting in warmer surface temperatures and enhanced convection, which were both much more realistic. Over South America, however, the reduction in cloud cover as a result of the ISCCP low-level cloud specification resulted in excessive net absorbed shortwave radiation at the top of the atmosphere, which was not entirely compensated for by a decrease in OLR. This, in turn, produced much warmer surface temperatures than are found in observations. Yet, this prescription was needed for a proper position of the Walker circulation (CMIOLE vs CMIOL). This points to a serious error in the CGCM's handling of the radiational and, perhaps, the diabatic processes in this region and thus will be the focus of continued research. Other work will investigate the effects of altered tropical land surface heating profiles on the strength and frequency of ENSO simulations in a long coupled model run. In addition, there are indications that a poor representation

of the position of the Walker circulation might affect the model-calculated statistical relationship between MJO and ENSO. If so, then it might be possible that a more reasonable positioning of the Walker circulation might give insight into the relationship between these two phenomena.

REFERENCES

Barkstrom, B. R., E. F. Harrison, and R. B. Lee III, 1990: Earth Radiation Budget Experiment, preliminary seasonal results. *Eos, Trans. Amer. Geophys. Union,* **71,** 297, 304–305.

Derber, J., and A. Rosati, 1989: A global oceanic data assimilation system. *J. Phys. Oceanogr.,* **19,** 1333–1347.

Gordon, C. T., A. Rosati, and R. Gudgel, 2000: Tropical sensitivity of a coupled model to specified ISCCP low clouds. *J. Climate,* **13,** 2239–2260.

Hahn, C. J., S. G. Warren, and J. London, 1996. Edited synoptic cloud reports from ships and land stations over the globe: 1982–1991. Tech. Rep. NDP026B, Carbon Dioxide Information Analysis Center, Oak Ridge National Laboratory, Oak Ridge, TN, 45 pp. [Available online at cdiac.esd.ornl.gov.]

Hughs, N. A., 1984: Global cloud climatologies: A historical review. *J Climate Appl. Meteor.,* **23,** 724–751.

Kiehl, J. T., 1998: Simulation of the tropical pacific warm pool with the NCAR climate system model. *J. Climate,* **11,** 1342–1355.

Legler, D. M., and J. J. O'Brien, 1988: Tropical Pacific wind stress analysis for TOGA, IOC time series of ocean measurements. Vol. 4, IOC Tech. Series, No. 33, UNESCO, 11–17.

Ma, C.-C., C. R. B. Mechoso, A. W. Robertson, and A. Arakawa, 1996: Peruvian stratus clouds and the tropical Pacific circulation: A coupled ocean–atmosphere GCM study. *J. Climate,* **9,** 1625–1645.

Mechoso, C. R., and Coauthors, 1995: The seasonal cycle over the tropical Pacific in coupled ocean–atmosphere general circulation models. *Mon. Wea. Rev.,* **123,** 2825–2838.

Meleshko, V. P., and R. T. Wetherald, 1981: The effect of a geographical cloud distribution on climate: A numerical experiment with an atmosphere general circulation model. *J. Geophys. Res.,* **86** (C12), 11 995–12 014.

Mokhov, I. I., and M. E. Schlesinger, 1994: Analysis of global cloudiness. 2. Comparisons of ground-based and satellite-based cloud climatologies. *J. Geophys. Res.,* **99,** 17 045–17 065.

Moorthi, S., and M. J. Suarez, 1992: Relaxed Arakawa–Schubert: A parameterization of moist convection for general circulation models. *Mon. Wea. Rev.,* **120,** 978–1002.

Newell, R. E., J. W. Kidson, D. G. Vincent, and G. J. Boer, 1974: *The General Circulation of the Tropical Atmosphere.* Massachusetts Institute of Technology/Colonial Press, 149 pp.

Pacanowski, R. C., 1995: MOM documentation user's guide and reference manual. GFDL Ocean Tech. Rep. 3, GFDL/NOAA, Princeton, NJ, 232 pp. [Available from NOAA/GFDL, P.O. Box 308, Princeton, NJ, 08542-0308.]

——, and S. G. H. Philander, 1981: Parameterization of vertical mixing in numerical models of tropical oceans. *J. Phys. Oceanogr.,* **11,** 1443–1451.

Reynolds, R. W., 1988: A real-time global sea surface temperature analysis. *J. Climate,* **1,** 75–86.

Rosati, A., R. Gudgel, and K. Miyakoda, 1994: Decadal analysis produced from an ocean data assimilation system. *Mon. Wea. Rev.,* **123,** 2206–2228.

——, K. Miyakoda, and R. Gudgel, 1997: The impact of ocean initial conditions on ENSO forecasting with a coupled model. *Mon. Wea. Rev.,* **125,** 754–772.

Rossow, W. B., A. Walker, and M. Roiter, 1996: International Satellite Cloud Climatology Project (ISCCP) description of reduced resolution radiance data, revised. WMO/TD-No. 58, World Meteorological Organization, 163 pp.

Smagorinsky, J., 1963: General circulation experiments with the primitive equations. Part 1: The basic experiment. *Mon. Wea. Rev.,* **91,** 99–164.

Stockdale, T., M. Latif, G. Burgers, and J.-O. Wolff, 1994: Some sensitivities of a coupled ocean–atmosphere GCM. *Tellus,* **46A,** 367–380.

Weare, B. C., 1999: Near-global observation of low clouds, *J. Climate,* **13,** 1255–1268.

Webster, P. J., 1994: The role of hydrological processes in ocean–atmosphere interactions. *Rev. Geophys.,* **32,** 427–476.

Wielicki, B. A., and L. Parker, 1992: On the determination of cloud cover from satellite sensors: The effect of sensor spatial resolution. *J. Geophys. Res.,* **97,** 12 799–12 823.

Yu, J.-Y., and C. R. Mechoso, 1999: Links between annual variations of Peruvian stratus clouds and of SST in the eastern equatorial Pacific. *J. Climate,* **12,** 3305–3318.